Condensed Matter Physics 2008, Vol. 11, No 3(55), pp. 495–507

CONDENSED MATTER PHYSICS

Electronic spectrum and superconductivity in Hubbard model*

N.M.Plakida[1,2], V.S.Oudovenko[1,3]

[1] Joint Institute for Nuclear Research, 141980 Dubna, Russia

[2] Max-Planck-Institut für Physik Komplexer Systeme, D–01187 Dresden, Germany

[3] Rutgers University, Piscataway, New Jersey 08854, USA

Received May 20, 2008, in final form June 10, 2008

A microscopic theory of electronic spectrum and superconducting pairing within the Hubbard model is formulated. The Dyson equation for the normal and anomalous Green functions in terms of the Hubbard operators is derived by applying the Mori-type projection technique. The self-energy is evaluated in the noncrossing approximation for electron scattering on spin and charge fluctuations induced by kinematic interaction for Hubbard operators. Numerical results for electron dispersion in the strong correlation limit are presented. Superconducting pairing mediated by antiferromagnetic exchange and spin fluctuations is discussed.

Key words: *strong electron correlations, Hubbard model, superconductivity*

PACS: *74.20.Mn, 71.27.+a, 71.10.Fd, 74.72.-h*

1. Introduction

One of the basic models for the study of electronic spectra and superconductivity in strongly correlated electronic systems, such as the cuprate high-temperature superconductors, is the Hubbard model [1]. In the simplest approximation the model is specified by two parameters: the single-electron hopping matrix element t between the nearest neighbors and the single-site Coulomb energy U:

$$H = -t \sum_{i \neq j \sigma} a^{\dagger}_{i\sigma} a_{j\sigma} + U \sum_{i} n_{i\uparrow} n_{i\downarrow} , \tag{1}$$

where $a^{\dagger}_{i\sigma}(a_{i\sigma})$ are the creation (annihilation) operators for electrons of spin σ at the lattice site i and $n_{i\sigma} = a^{\dagger}_{i\sigma} a_{i\sigma}$ is the electron occupation number. The model (1) permits to consider both the cases of weak correlations, $U \ll W$, and of strong correlations, $U \gg W$, where $W = 2zt$ is the bandwidth (z is the number of the nearest neighbors). In the weak correlation limit a metallic state is observed, while in the strong correlation limit the model describes a Mott-Hubbard insulating state at half-filling (an average occupation electron number $n = 1$). For hole doping ($n < 1$) of the lower Hubbard subband (LHB), or for electron doping ($n > 1$) of the upper Hubbard subband (UHB) the model describes a strongly correlated metal.

While investigating the Hubbard model various methods have been used such as numerical simulations for finite clusters (for a review see [2,3]), dynamical mean field theory (DMFT) (for a review see [4,5]), the dynamical cluster theory (for a review see [6,7]), etc. (see [8] and references therein). A rigorous analytical method is based on the Hubbard operator (HO) technique [9] since in this representation the local constraint of no double occupancy of any lattice site is rigorously implemented by the Hubbard operator algebra. A superconducting pairing due to the kinematic interaction in the Hubbard model in the limit of strong electron correlations ($U \to \infty$) was first obtained by Zaitsev and Ivanov [10] who studied the two-particle vertex equation by applying a diagram technique for Hubbard operators. However, they studied only the lowest order diagrams

*The paper is dedicated to the 70-th birthday of Professor I.V. Stasyuk

which are equivalent to the mean-field approximation (MFA) for a superconducting order parameter and obtained only the **k**-independent s-wave pairing. Subsequently, superconducting pairing in the Hubbard model was studied by Plakida and Stasyuk [11] by applying the equation of motion method to the thermodynamic Green functions (GFs) [12]. They have used a decoupling procedure for higher order GFs in MFA and obtained the results similar to [10] but with a different dependence of the superconducting temperature $T_c(n)$ on the electron occupations numbers n. As was found later in the study of the t-J model within the Mori-type projection technique [13], in the simple decoupling procedure used in [11] commutation relations specific for HOs were not properly taken into account which resulted in a different formula for $T_c(n)$ in comparison with [10]. A self-consistent solution of Dyson equations for normal and anomalous GFs and respective self-energies within the t-J model was performed in [14] which confirmed the results of the previous studies in MFA [13].

There are several later studies of superconductivity in the Hubbard model within the MFA [15–17], where, however, a spin-fluctuation channel of superconducting pairing resulting from the anomalous component of the self-energy was not taken into account. Electronic spectra for the effective p-d Hubbard model in MFA was calculated in [18], while self-energy effects on electronic spectra were studied in [19] based on a self-consistent solution of the Dyson equations for GFs and the self-energy. A general formulation of a superconductivity theory within the Dyson equation for the normal and anomalous GFs in the Hubbard model was given in [20]. A weak-coupling approximation in the theory was considered in [21] where $T_c(n)$ dependence was calculated and the d-wave symmetry of the superconducting gap was confirmed.

In the present paper a consistent microscopic theory for electronic spectra and superconductivity in the strongly correlated limit of the Hubbard model is formulated. The theory is based on the solution of the Dyson equation for the thermodynamic GFs in terms of HOs with a self-energy evaluated in the noncrossing approximation (NCA). We present several numerical results for electronic spectra for parameters of the Hubbard model different from those considered in [19] and formulate superconducting equations with due regard for the two-band nature of the Hubbard model in the limit of strong correlations.

In the next section we briefly discuss the model and derivation of the Dyson equation and self-energy in NCA. A self-consistent system of equations for a hole-doped case is considered in section 3 where several results of numerical calculations for electronic spectra and T_c are presented. Concluding remarks are given in section 4.

2. General formulation

2.1. Hubbard model

We consider a Hubbard model on a square lattice in a hole representation usually used in describing cuprate superconductors:

$$H = E_1 \sum_{i,\sigma} X_i^{\sigma\sigma} + E_2 \sum_i X_i^{22} + \sum_{i\neq j,\sigma} t_{ij}\{X_i^{\sigma 0} X_j^{0\sigma} + X_i^{2\sigma} X_j^{\sigma 2} + \sigma(X_i^{2\bar{\sigma}} X_j^{0\sigma} + \text{H.c.})\}, \qquad (2)$$

where $X_i^{\alpha\beta} = |i\alpha\rangle\langle i\beta|$ are HOs for the four states $\alpha, \beta = |0\rangle, |\sigma\rangle, |2\rangle = |\uparrow\downarrow\rangle$, $\sigma = \pm 1 = (\uparrow, \downarrow)$, $\bar{\sigma} = -\sigma$. We denote the single-site repulsion energy by U and introduce $E_1 = \varepsilon_1 - \mu$ and $E_2 = 2E_1 + U$ as the energy levels for the one-hole (with a reference energy ε_1) and the two-hole states. The model (2) can be used to study cuprate superconductors by setting $U = \Delta_{pd}$ where Δ_{pd} is the charge-transfer gap in cuprates. In this case the one-hole band is the d-like copper band ($\varepsilon_1 = \varepsilon_d$) and the two-hole band is the Zhang-Rice (ZR) p-d singlet band ($\varepsilon_2 = \varepsilon_d + \varepsilon_p$) [22] (see, e.g., [23]).

The bare electron dispersion is defined by the hopping parameter t_{ij} which **k**-dependence is specified by the equation

$$t(\mathbf{k}) = 4t\,\gamma(\mathbf{k}) + 4t'\,\gamma'(\mathbf{k}) + 4t''\,\gamma''(\mathbf{k}), \qquad (3)$$

where the hopping parameters are equal to t for the nearest neighbors and t', t'' for the second neighbors, which determine the bare (band) dispersion by the functions: $\gamma(\mathbf{k}) = (1/2)(\cos k_x +$

$\cos k_y$), $\gamma'(\mathbf{k}) = \cos k_x \cos k_y$ and $\gamma''(\mathbf{k}) = (1/2)(\cos 2k_x + \cos 2k_y)$. The chemical potential μ depends on the average *hole* occupation number

$$n = \langle N_i \rangle, \quad N_i = \sum_\sigma X_i^{\sigma\sigma} + 2X_i^{22}, \tag{4}$$

where $\langle \ldots \rangle$ denotes the statistical average. The spin operators in terms of HOs are defined as

$$S_i^\sigma = X_i^{\sigma\bar{\sigma}}, \qquad S_i^z = (1/2) \sum_\sigma \sigma \, X_i^{\sigma\sigma}. \tag{5}$$

The HOs satisfy the completeness relation $X_i^{00} + X_i^{\uparrow\uparrow} + X_i^{\downarrow\downarrow} + X_i^{22} = 1$ and the multiplication rules $X_i^{\alpha\beta} X_i^{\gamma\delta} = \delta_{\beta\gamma} X_i^{\alpha\delta}$. From the latter follow the commutation relations

$$\left[X_i^{\alpha\beta}, X_j^{\gamma\delta} \right]_\pm = \delta_{ij} \left(\delta_{\beta\gamma} X_i^{\alpha\delta} \pm \delta_{\delta\alpha} X_i^{\gamma\beta} \right). \tag{6}$$

The upper sign pertains to Fermi-type operators like $X_i^{0\sigma}$ which change a number of particles and the lower sign pertains to Bose-type operators, for example, the particle number operator N_i in (4) or spin operators S_i^α (5).

We emphasize here that the Hubbard model (2) does not involve a dynamical coupling of electrons (holes) to fluctuations of spins or charges. Its role is played by the *kinematic* interaction caused by the non-Fermi nature of commutation relations (6) for the HOs, as was already noted by Hubbard [9]. For example, the equation of motion for the HO $X_i^{\sigma 2}$ has the form

$$\begin{aligned} \mathrm{i}\, \mathrm{d}X_i^{\sigma 2}/\mathrm{d}t &= [X_i^{\sigma 2}, H] = (E_1 + U) X_i^{\sigma 2} \\ &+ \sum_{l \neq i, \sigma'} t_{il} \left(B_{i\sigma\sigma'}^{22} X_l^{\sigma' 2} - \sigma B_{i\sigma\sigma'}^{21} X_l^{0\bar{\sigma}'} \right) - \sum_{l \neq i} t_{il} \, X_i^{02} \left(X_l^{\sigma 0} + \sigma X_l^{2\bar{\sigma}} \right), \end{aligned} \tag{7}$$

$$B_{i\sigma\sigma'}^{22} = (X_i^{22} + X_i^{\sigma\sigma}) \, \delta_{\sigma'\sigma} + X_i^{\sigma\bar{\sigma}} \, \delta_{\sigma'\bar{\sigma}} = (N_i/2 + S_i^z) \, \delta_{\sigma'\sigma} + S_i^\sigma \, \delta_{\sigma'\bar{\sigma}},$$

$$B_{i\sigma\sigma'}^{21} = (N_i/2 + S_i^z) \, \delta_{\sigma'\sigma} - S_i^\sigma \, \delta_{\sigma'\bar{\sigma}}. \tag{8}$$

Here $B_{i\sigma\sigma'}^{\alpha\beta}$ are Bose-like operators related to the particle number operator N_i and spin operators S_i^α (5).

2.2. Dyson equation

To consider the superconducting pairing in Hubbard model (2), we define the thermodynamic anticommutator GF as a 4×4 matrix in Zubarev notation [12]:

$$\mathsf{G}_{ij\sigma}(\omega) = \langle\langle \hat{X}_{i\sigma} \mid \hat{X}_{j\sigma}^\dagger \rangle\rangle_\omega = \begin{pmatrix} \hat{G}_{ij\sigma}(\omega) & \hat{F}_{ij\sigma}(\omega) \\ \hat{F}_{ij\sigma}^\dagger(\omega) & -\hat{G}_{ji\bar{\sigma}}(-\omega) \end{pmatrix}, \tag{9}$$

where we introduce the four-component Nambu operator $\hat{X}_{i\sigma}$ and its conjugate operator $\hat{X}_{i\sigma}^\dagger = (X_i^{2\sigma} \; X_i^{\bar{\sigma}0} \; X_i^{\bar{\sigma}2} \; X_i^{0\sigma})$. Due to the two-subband nature of the model (2), the normal $\hat{G}_{ij\sigma}$ and anomalous $\hat{F}_{ij\sigma}$ components of the GF are 2×2 matrices which are coupled by the symmetry relations for the anticommutator retarded GF [12].

To calculate the GF (9) we use the method of the equations of motion. Differentiating the GF with respect to the time t, its Fourier representation leads to the equation

$$\omega \mathsf{G}_{ij\sigma}(\omega) = \delta_{ij} \mathsf{Q} + \langle\langle [\hat{X}_{i\sigma}, H] \mid \hat{X}_{j\sigma}^\dagger \rangle\rangle_\omega, \tag{10}$$

$$\text{where} \qquad \mathsf{Q} = \langle \{ \hat{X}_{i\sigma}, \hat{X}_{i\sigma}^\dagger \} \rangle = \hat{\tau}_0 \times \hat{Q}, \quad \hat{Q} = \begin{pmatrix} Q_2 & 0 \\ 0 & Q_1 \end{pmatrix}. \tag{11}$$

Here $\hat{\tau}_0$ is the 2×2 unit matrix and in a paramagnetic state the coefficients $Q_2 = \langle X_i^{22} + X_i^{\sigma\sigma} \rangle = n/2$ and $Q_1 = \langle X_i^{00} + X_i^{\bar{\sigma}\bar{\sigma}} \rangle = 1 - Q_2$ depend only on the occupation number of holes (4). In

the Q matrix we neglect anomalous averages of the type $\langle X_i^{02}\rangle$ which give no contribution to the d-wave pairing.

In the Hubbard model, there are no well-defined QP excitations specified by zeroth-order kinetic energy. Therefore, it is convenient to choose the mean-field contribution to the energy of QPs in the equations of motion (10) as the zeroth-order QP energy. To identify this contribution, we use the Mori-type projection method. To this end, we write the operator $\hat{Z}_{i\sigma} = [\hat{X}_{i\sigma}, H]$ in (10) as a sum of the linear part, proportional to the original operator $\hat{X}_{i\sigma}$, and the irreducible part $\hat{Z}^{(\mathrm{ir})}_{i\sigma}$ orthogonal to $\hat{X}_{i\sigma}$:

$$\hat{Z}_{i\sigma} = [\hat{X}_{i\sigma}, H] = \sum_l \mathsf{E}_{il\sigma}\hat{X}_{l\sigma} + \hat{Z}^{(\mathrm{ir})}_{i\sigma}. \tag{12}$$

The orthogonality conditions $\langle\{\hat{Z}^{(\mathrm{ir})}_{i\sigma}, \hat{X}^\dagger_{j\sigma}\}\rangle = \langle\hat{Z}^{(\mathrm{ir})}_{i\sigma}\hat{X}^\dagger_{j\sigma} + \hat{X}^\dagger_{j\sigma}\hat{Z}^{(\mathrm{ir})}_{i\sigma}\rangle = 0$ determine the linear part, the frequency matrix:

$$\mathsf{E}_{ij\sigma} = \left\langle \left\{ [\hat{X}_{i\sigma}, H], \hat{X}^\dagger_{j\sigma} \right\} \right\rangle \mathsf{Q}^{-1}. \tag{13}$$

Frequency matrix (13) determines QP spectrum in the generalized MFA and the corresponding zeroth-order GF. Passing to the Fourier representation in the $(\mathbf{q}, \omega)$ space, we write the zeroth-order GF as

$$\mathsf{G}^0_\sigma(\mathbf{q}, \omega) = \Big(\omega\tilde{\tau}_0 - \mathsf{E}_\sigma(\mathbf{q})\Big)^{-1}\mathsf{Q}\,, \tag{14}$$

where $\tilde{\tau}_0$ is the 4×4 unit matrix.

Differentiating the multiparticle GF $\langle\langle \hat{Z}_{i\sigma}(t) \mid \hat{X}^\dagger_{j\sigma}(t')\rangle\rangle$ in (10) with respect to the second time t' and using the same projection procedure as in (12) leads to the Dyson equation for the GF (9). In the $(\mathbf{q}, \omega)$-representation, the Dyson equation becomes

$$(\mathsf{G}_\sigma(\mathbf{q}, \omega))^{-1} = \big(\mathsf{G}^0_\sigma(\mathbf{q}, \omega)\big)^{-1} - \mathsf{\Sigma}_\sigma(\mathbf{q}, \omega). \tag{15}$$

The self-energy operator $\mathsf{\Sigma}_\sigma(\mathbf{q}, \omega)$ is defined by the *proper* part of the scattering matrix

$$\mathsf{\Sigma}_\sigma(\mathbf{q}, \omega) = \mathsf{Q}^{-1}\langle\!\langle \hat{Z}^{(\mathrm{ir})}_{\mathbf{q}\sigma} \mid \hat{Z}^{(\mathrm{ir})\dagger}_{\mathbf{q}\sigma}\rangle\!\rangle^{(\mathrm{prop})}_\omega\ \mathsf{Q}^{-1}. \tag{16}$$

Dyson equations (13)–(16) give an exact representation for GF (9). To obtain a closed system of equations, we must evaluate the multiparticle GF in self-energy operator (16); this describes the processes of inelastic scattering of electrons (holes) on charge and spin fluctuations due to kinematic interaction.

2.3. Mean-field approximation

The superconducting pairing in the Hubbard model already occurs in the MFA and is caused by the kinetic exchange interaction as proposed by Anderson [24]. Therefore it is reasonable to consider the MFA described by zeroth-order GF (14) separately. Using commutation relations for Hubbard operators (6), we evaluate the frequency matrix (13):

$$\mathsf{E}_{ij\sigma} = \begin{pmatrix} \hat{\varepsilon}_{ij\sigma} & \hat{\Delta}_{ij\sigma} \\ \hat{\Delta}^*_{ji\sigma} & -\hat{\varepsilon}_{ji\bar{\sigma}} \end{pmatrix}, \quad \text{or} \quad \mathsf{E}_\sigma(\mathbf{k}) = \begin{pmatrix} \hat{\varepsilon}_\sigma(\mathbf{k}) & \hat{\Delta}_\sigma(\mathbf{k}) \\ \hat{\Delta}^*_\sigma(\mathbf{k}) & -\hat{\varepsilon}_{\bar{\sigma}}(\mathbf{k}) \end{pmatrix}. \tag{17}$$

The matrix $\hat{\varepsilon}_\sigma(\mathbf{k})$ determines the QP spectrum in the two Hubbard bands in the normal phase (for details see [18,19])

$$\begin{aligned} \varepsilon_{1,2}(\mathbf{k}) &= (1/2)[\omega_2(\mathbf{k}) + \omega_1(\mathbf{k})] \mp (1/2)\Lambda(\mathbf{k}), \\ \Lambda(\mathbf{k}) &= \{[\omega_2(\mathbf{k}) - \omega_1(\mathbf{k})]^2 + 4W(\mathbf{k})^2\}^{1/2}, \end{aligned} \tag{18}$$

where $\omega_1(\mathbf{k}) = 4t\,\alpha_1\gamma(\mathbf{k}) + 4t'\,\beta_1\gamma'(\mathbf{k}) - \mu$, $\omega_2(\mathbf{k}) = 4t\,\alpha_2\gamma(\mathbf{k}) + 4t'\,\beta_2\gamma'(\mathbf{k}) + U - \mu$, and $W(\mathbf{k}) = 4t\,\alpha_{12}\gamma(\mathbf{k}) + 4t'\,\beta_{12}\gamma'(\mathbf{k})$. Due to the kinematic interaction, the spectrum is renormalized: $\alpha_{1(2)} =$

$Q_{1(2)}[1+C_1/Q^2_{1(2)}]$, $\beta_{1(2)}=Q_{1(2)}[1+C_2/Q^2_{1(2)}]$, $\alpha_{12}=\sqrt{Q_1Q_2}[1-C_1/Q_1Q_2]$, $\beta_{12}=\sqrt{Q_1Q_2}[1-C_2/Q_1Q_2]$. Here, beyond the Hubbard I renormalization of hopping parameters given by the factors $Q_{1(2)}$, we take into consideration the renormalization caused by spin correlation functions for the nearest and the second neighbors, respectively:

$$C_1=\langle \mathbf{S}_i\mathbf{S}_{i\pm a_x/a_y}\rangle, \qquad C_2=\langle \mathbf{S}_i\mathbf{S}_{i\pm a_x\pm a_y}\rangle\,. \tag{19}$$

They considerably suppress the hopping parameters for the nearest neighbors: $\alpha_{1(2)}\ll 1$ since due to AF correlations $C_1<0, |C_1|=0.1-0.2$. However, we neglect charge correlations in the renormalization by using the approximation $\langle N_iN_j\rangle=\langle N_i\rangle\langle N_j\rangle$. For a moderate Coulomb energy $U\leqslant 8t$, charge fluctuations may be important in reducing strong renormalization caused by AF spin correlations.

Now we evaluate the anomalous component $\hat{\Delta}_{ij\sigma}$ of matrix (17), which determines the superconducting gap. In what follows, we consider only the singlet d-type pairing, which is determined by the anomalous averages at noncoincident sites, $(i\neq j)$. The diagonal matrix components have the forms

$$\Delta^{22}_{ij\sigma}=-\sigma t_{ij}\langle X^{02}_iN_j\rangle/Q_2\,, \qquad \Delta^{11}_{ij\sigma}=\sigma t_{ij}\langle N_jX^{02}_i\rangle/Q_1\,. \tag{20}$$

Expressing the Fermi operators in terms of the Hubbard operators as $a_{i\sigma}=X^{0\sigma}_i+\sigma X^{\bar\sigma 2}_i$, we can write the anomalous averages in (20) as $\langle a_{i\downarrow}\,a_{i\uparrow}N_j\rangle=\langle X^{0\downarrow}_iX^{\downarrow 2}_iN_j\rangle=\langle X^{02}_iN_j\rangle$, because the other products of the Hubbard operators do not contribute, in accordance with the multiplication rules, $X^{\alpha\gamma}_iX^{\lambda\beta}_i=\delta_{\gamma,\lambda}X^{\alpha\beta}_i$. This representation of the anomalous averages in terms of Fermi operators shows that the pairing occurs at a single site but in different Hubbard subbands.

The anomalous averages $\langle X^{02}_iN_j\rangle$ can be calculated directly by using the equation for the pair commutator GF $L_{ij}(t-t')=\langle\langle X^{02}_i(t)\mid N_j(t')\rangle\rangle$ without *any decoupling* approximations [21]. Here we present only the result for the correlation function for the two-hole band, in which the pairing occurs under the hole doping, $n=1+\delta>1$:

$$\langle X^{02}_iN_j\rangle=-\frac{1}{U}\sum_{m\neq i,\sigma}\sigma t_{im}\langle X^{\sigma 2}_iX^{\bar\sigma 2}_mN_j\rangle\simeq-\frac{4t_{ij}}{U}\sigma\,\langle X^{\sigma 2}_iX^{\bar\sigma 2}_j\rangle. \tag{21}$$

The last equation is obtained in the two-site approximation, $m=j$, which is typically used to derive the t-J model. As a result, the equation for the superconducting gap in formulas (20) in the case of hole doping can be written as

$$\Delta^{22}_{ij\sigma}=-\sigma\,t_{ij}\langle X^{02}_iN_j\rangle/Q_2=J_{ij}\langle X^{\sigma 2}_iX^{\bar\sigma 2}_j\rangle/Q_2\,. \tag{22}$$

The obtained equation is equivalent to the gap equation in the t-J model, leading to a pairing due to the exchange interaction $J_{ij}=4\,(t_{ij})^2/U$ [13]. A similar equation can also be obtained in the case of electron doping for the gap in the one-hole Hubbard band: $\Delta^{11}_{ij\sigma}=J_{ij}\,\langle X^{0\bar\sigma}_iX^{0\sigma}_j\rangle/Q_1$. Thus we conclude that anomalous averages (20) in the Hubbard model correspond to the anomalous averages in one of the Hubbard subbands (depending on the position of the chemical potential) in the t-J model. Therefore, this is just conventional pairing mediated by the exchange interaction which has been extensively studied within the t-J model (see, e.g., [13,14] and references therein).

The same anomalous pair correlation functions (20) were obtained in MFA for the original Hubbard model (1) in [15–17]. To calculate the anomalous correlation function $\langle c_{i\downarrow}c_{i\uparrow}N_j\rangle$ in [15,17] the Roth procedure was used based on a decoupling of the operators on the same lattice site in the time-dependent correlation function: $\langle c_{i\downarrow}(t)|c_{i\uparrow}(t')N_j(t')\rangle$. However, the decoupling of the Hubbard operators on the same lattice site is not unique (as has been really observed in [15,17]) and unreliable. To escape uncontrollable decoupling, in [16] kinematical restrictions imposed on the correlation functions for the Hubbard operators were used which, however, also have not produced a unique solution for superconducting equations.

2.4. Self-energy operator

Self-energy operator (16) can be conveniently written in the same form as GF (9):

$$\Sigma_{ij\sigma}(\omega) = \mathsf{Q}^{-1} \begin{pmatrix} \hat{M}_{ij\sigma}(\omega) & \hat{\Phi}_{ij\sigma}(\omega) \\ \hat{\Phi}^{\dagger}_{ij\sigma}(\omega) & -\hat{M}_{ji\bar{\sigma}}(-\omega) \end{pmatrix} \mathsf{Q}^{-1}, \tag{23}$$

where the matrices $\hat{M}$ and $\hat{\Phi}$ denote the respective normal and anomalous components of the self-energy operator.

The system of equations for the (4×4) matrix GF (9) and the self-energy (23) can be reduced to a system of equations for the normal $\hat{G}_\sigma(\mathbf{k},\omega)$ and anomalous $\hat{F}_\sigma(\mathbf{k},\omega)$ (2×2) matrix components. By using representations for the frequency matrix (17) and the self-energy (23), we derive for these components the following system of matrix equations:

$$\hat{G}_\sigma(\mathbf{k},\omega) = \left(\hat{G}_N(\mathbf{k},\omega)^{-1} + \hat{\varphi}_\sigma(\mathbf{k},\omega)\,\hat{G}_N(\mathbf{k},-\omega)\,\hat{\varphi}^*_\sigma(\mathbf{k},\omega)\right)^{-1}\hat{Q}, \tag{24}$$

$$\hat{F}^*_\sigma(\mathbf{k},\omega) = -\hat{G}_N(\mathbf{k},-\omega)\,\hat{\varphi}^*_\sigma(\mathbf{k},\omega)\,\hat{G}_\sigma(\mathbf{k},\omega). \tag{25}$$

In (24) we introduced the normal state matrix GF and the matrix superconducting gap function:

$$\hat{G}_N(\mathbf{k},\omega) = \left(\omega\hat{\tau}_0 - \hat{\varepsilon}(\mathbf{k}) - \hat{M}(\mathbf{k},\omega)/\hat{Q}\right)^{-1}, \tag{26}$$

$$\hat{\varphi}_\sigma(\mathbf{k},\omega) = \hat{\Delta}_\sigma(\mathbf{k}) + \hat{\Phi}_\sigma(\mathbf{k},\omega)/\hat{Q}. \tag{27}$$

To calculate the self-energy matrix (16) we use the non-crossing (NCA) or the self-consistent Born approximation (SCBA). In this approximation, Fermi-like excitations described by operators $X_j = X_j^{0\sigma}$ $(X_j^{\bar{\sigma}2})$ and Bose-like excitations described by operators B_i (8) in multiparticle GF (16) are considered to propagate independently, and therefore their correlation functions at noncoincident lattice sites $(i \neq j,\, l \neq m)$ factor into a product of the corresponding functions:

$$\langle B_i(t)X_j(t)B_l(t')X_m(t')\rangle \simeq \langle X_j(t)X_m(t')\rangle\langle B_i(t)B_l(t')\rangle. \tag{28}$$

Using the spectral representation for these correlation functions we get in the NCA the following expressions for the normal $M^{\alpha\alpha}_\sigma(\mathbf{q},\omega)$ and anomalous $\Phi^{\alpha\alpha}_\sigma(\mathbf{q},\omega)$ diagonal components of the self-energy:

$$M^{22}_\sigma(\mathbf{k},\omega) = \frac{1}{N}\sum_{\mathbf{q}}\int_{-\infty}^{+\infty}\mathrm{d}z\, K^{(+)}(\omega,z|\mathbf{q},\mathbf{k}-\mathbf{q})\left\{-\frac{1}{\pi}\mathrm{Im}\left[G^{22}_\sigma(\mathbf{q},z) + G^{11}_\sigma(\mathbf{q},z)\right]\right\}, \tag{29}$$

$$\Phi^{22}_\sigma(\mathbf{k},\omega) = \frac{1}{N}\sum_{\mathbf{q}}\int_{-\infty}^{+\infty}\mathrm{d}z\, K^{(-)}(\omega,z|\mathbf{q},\mathbf{k}-\mathbf{q})\left\{-\frac{1}{\pi}\mathrm{Im}\left[F^{22}_\sigma(\mathbf{q},z) - F^{11}_\sigma(\mathbf{q},z)\right]\right\}, \tag{30}$$

where $G^{\alpha\alpha}_\sigma(\mathbf{q},z)$ and $F^{\alpha\alpha}_\sigma(\mathbf{q},z)$ are given by the diagonal components of the matrices (24), (25). Analogous expressions hold for $M^{11}_\sigma(\mathbf{k},\omega)$ and $\Phi^{11}_\sigma(\mathbf{k},\omega)$ [20] . The kernel of the integral equations (29), (30) has a form, similar to the strong coupling Eliashberg theory [25]:

$$K^{(\pm)}(\omega,z|\mathbf{q},\mathbf{k}-\mathbf{q}) = |t(\mathbf{q})|^2\,\frac{1}{2\pi}\int_{-\infty}^{+\infty}\frac{\mathrm{d}\Omega}{\omega - z - \Omega}\left[\tanh\frac{z}{2T} + \coth\frac{\Omega}{2T}\right]\mathrm{Im}\,\chi^{(\pm)}_{\mathrm{sc}}(\mathbf{k}-\mathbf{q},\Omega), \tag{31}$$

where the interaction is defined by the hopping parameter $t(\mathbf{q})$ (3). The spectral density of bosonic excitations in (31) is determined by the dynamic susceptibility of the Bose-like operators $B_i(t)$ – the spin and number (charge) fluctuations:

$$\chi^{(\pm)}_{\mathrm{sc}}(\mathbf{q},\omega) = \chi_s(\mathbf{q},\omega) \pm \chi_c(\mathbf{q},\omega) = -[\langle\langle \mathbf{S}_\mathbf{q}|\mathbf{S}_{-\mathbf{q}}\rangle\rangle_\omega \pm (1/4)\langle\langle \delta N_\mathbf{q}|\delta N_{-\mathbf{q}}\rangle\rangle_\omega], \tag{32}$$

where we introduced the commutator GF for the spin $\mathbf{S_q}$ and the number $\delta N_{\mathbf{q}} = N_{\mathbf{q}} - \langle N_{\mathbf{q}} \rangle$ operators. The renormalized QP spectrum in the two-hole subband in the normal state is determined by the equation (26): $\tilde{\varepsilon}_2(\mathbf{k}) \simeq \varepsilon_2(\mathbf{k}) + \mathrm{Re}M^{22}_{\sigma}(\mathbf{q}, \omega = \tilde{\varepsilon}_2(\mathbf{k}))/Q_2$, while the gap function (27) is defined as $\varphi_{2,\sigma}(\mathbf{k}, \omega) = \Delta^{22}_{\sigma}(\mathbf{k}) + \Phi^{22}_{\sigma}(\mathbf{k}, \omega)/Q_2$.

In the NCA vertex, corrections are neglected as in the Migdal-Eliashberg theory. For the electron-phonon system the vertex corrections are small in the adiabatic approximation, as shown by Migdal [26]. The kinematic interaction induced by the intraband hopping is of the same order as the bandwidth and vertex corrections may be important in obtaining quantitative results. However, in the NCA the self-energy is calculated self-consistently allowing to consider a strong coupling limit which plays an essential role both in renormalization of quasiparticle spectra and in superconducting pairing. Thus, this approach can be considered as a first reasonable approximation. Concerning the spin fluctuation contribution, it should be pointed out that the NCA is quite reliable in this case since a certain set of diagrams, in particular the first crossing diagram [27], vanishes due to kinematic restrictions for spin scattering processes.

3. Numerical results

In this section we consider a self–consistent system of equations for the GFs (24)–(27) and the self-energy (29), (30) for the two-hole subband at hole doping when $n = 1 + \delta > 1$. The normal GF (26) can be approximately written as

$$G^{22}_N(\mathbf{k}, \omega) = [1 - b(\mathbf{k})]G_2(\mathbf{k}, \omega) + b(\mathbf{k})G_1(\mathbf{k}, \omega), \tag{33}$$

$$G_{1(2)}(\mathbf{k}, \omega) = \frac{1}{\omega - \varepsilon_{1(2)}(\mathbf{k}) - \Sigma(\mathbf{k}, \omega)}, \tag{34}$$

where the hybridization parameter $b(\mathbf{k}) = [\varepsilon_2(\mathbf{k}) - \omega_2(\mathbf{k})]/[\varepsilon_2(\mathbf{k}) - \varepsilon_1(\mathbf{k})]$. The self-energy in (34) can be approximated by the same diagonal component for the both subbands:

$$\Sigma(\mathbf{k}, \omega) = \frac{1}{N} \sum_{\mathbf{q}} \int_{-\infty}^{+\infty} \mathrm{d}z K^{(+)}(\omega, z|\mathbf{q}, \mathbf{k} - \mathbf{q}) \Big(-\frac{1}{\pi} \mathrm{Im}[G_1(\mathbf{q}, z) + G_2(\mathbf{q}, z)] \Big). \tag{35}$$

The gap equation (27) for the diagonal component for the two-hole subband can be written as

$$\varphi_{2,\sigma}(\mathbf{k}, \omega) = \frac{1}{NQ_2} \sum_{\mathbf{q}} \int_{-\infty}^{+\infty} \mathrm{d}z \left[J(\mathbf{k} - \mathbf{q}) \frac{1}{2} \tanh \frac{z}{2T} + K^{(-)}(\omega, z|\mathbf{q}, \mathbf{k} - \mathbf{q}) \right] \left(-\frac{1}{\pi} \right) \mathrm{Im} F^{22}_{\sigma}(\mathbf{q}, z). \tag{36}$$

Here the gap equation (22) in MFA for the exchange interaction $J(\mathbf{q}) = 4J\gamma(\mathbf{q})$ was used where J is the exchange energy for the nearest neighbor spins. In (36) a contribution from the one-hole subband $F^{11}_{\sigma}(\mathbf{q}, z)$ was neglected since the gap function in this filled band much below the Fermi level is vanishingly small. To determine the superconducting T_{c} it is sufficient to solve a linear equation for the gap (36) by using the linearized anomalous GF (25):

$$F^{22}_{\sigma}(\mathbf{k}, \omega) = -G^{22}_N(\mathbf{k}, -\omega)\, \varphi_{2,\sigma}(\mathbf{k}, \omega)\, G^{22}_N(\mathbf{k}, \omega)\, Q_2 . \tag{37}$$

To solve the system of equations we should specify a model for the spin-charge susceptibility (32) in the kernel (31). Below we take into account only the spin-fluctuation contribution $\chi_s(\mathbf{q}, \omega) = -\langle\langle \mathbf{S}_q \mid \mathbf{S}_{-q} \rangle\rangle_{\omega}$ for which we adopt a model suggested in numerical studies [28]

$$\mathrm{Im}\, \chi_s(\mathbf{q}, \omega + \mathrm{i}0^+) = \chi_s(\mathbf{q})\, \chi_s^{''}(\omega) = \frac{\chi_0}{1 + \xi^2(1 + \gamma(\mathbf{q}))} \tanh \frac{\omega}{2T} \frac{1}{1 + (\omega/\omega_s)^2}. \tag{38}$$

The $\mathbf{q}$-dependence in $\chi_s(\mathbf{q})$ is determined by the AF correlation length ξ while a frequency dependence is determined by a continuous spin-fluctuation spectrum in $\chi_s^{''}(\omega)$ with a cut-off energy

of the order of the exchange energy $\omega_s \sim J$. The two fitting parameters, however, do not fix the strength of the spin-fluctuation interaction given by the static susceptibility χ_0 at the AF wave vector $\mathbf{Q} = (\pi, \pi)$. This parameter is fixed by the normalization condition:

$$\langle \mathbf{S}_i^2 \rangle = \frac{1}{N} \sum_i \langle \mathbf{S}_i \mathbf{S}_i \rangle = \frac{1}{\pi} \int_{-\infty}^{+\infty} \frac{\mathrm{d}z}{\exp(z/T) - 1} \chi_s''(z) \, \frac{1}{N} \sum_{\mathbf{q}} \chi_s(\mathbf{q}), \tag{39}$$

which gives the following value for this constant: $\chi_0 = (2\langle \mathbf{S}_i^2 \rangle / \omega_s)\{(1/N) \sum_{\mathbf{q}} 1/[1+\xi^2(1+\gamma(\mathbf{q}))]\}^{-1}$. In (39) we introduced $\langle \mathbf{S}_i^2 \rangle = (3/4)(1-|\delta|)$ where at the hole doping $\delta \simeq \langle X_i^{22} \rangle$, while at the electron doping $\delta \simeq -\langle X_i^{00} \rangle$.

The spin correlation functions (19) in the single-particle excitation spectra (18) in MFA are defined by equations

$$C_1 = \frac{1}{N} \sum_{\mathbf{q}} C_{\mathbf{q}} \, \gamma(\mathbf{q}), \qquad C_2 = \frac{1}{N} \sum_{\mathbf{q}} C_{\mathbf{q}} \, \gamma'(\mathbf{q}). \tag{40}$$

The static correlation function $C_{\mathbf{q}}$ can be calculated from the same model (38) as follows $C_{\mathbf{q}} = \langle \mathbf{S}_{\mathbf{q}} \mathbf{S}_{-\mathbf{q}} \rangle = C(\xi)/[1 + \xi^2(1 + \gamma(\mathbf{q}))]$, where the factor $C(\xi) = \chi_0 \, (\omega_s/2)$.

The doping dependence of the AF correlation length $\xi(\delta)$ at low temperature was evaluated from comparison of the correlation function C_1 calculated from (40) with numerical results of an exact diagonalization for finite clusters [29]. It was found that $\xi = 3 - 2$ for $\delta = 0.05 - 0.15$.

Below we discuss electronic spectra in the normal state in the hole-doped case and consider an equation for the superconducting gap in the two-subband model. An extensive study of dispersion of single-particle excitations, spectral functions, and the Fermi surface in the normal state have been reported in [19] in the limit of strong correlation for $U = 8t$. Here we present some of the numerical results for a modest correlation limit for $U = 4t$. The model dispersion (3) is specified by the hoping parameters $t' = -0.13t$, $t'' = 016t$ suggested for a model of La_2CuO_4 in [30].

3.1. Normal state electronic spectrum

The spectrum of single-electron excitations is determined by the spectral function $A_{(\mathrm{el})}(\mathbf{k}, \omega) = A_{(h)}(\mathbf{k}, -\omega)$ where the spectral function for single-hole excitations is determined as

$$A_{(h)}(\mathbf{k}, \omega) = [Q_1 + P(\mathbf{k})][-(1/\pi) \operatorname{Im} G_1(\mathbf{k}, \omega)] + [Q_2 - P(\mathbf{k})][-(1/\pi)] \operatorname{Im} G_2(\mathbf{k}, \omega), \tag{41}$$

where the parameter $P(\mathbf{k}) = (n-1)b(\mathbf{k}) - 2\sqrt{Q_1 \, Q_2} \, W(\mathbf{k})/\Lambda(\mathbf{k})$ takes into account hybridization effects both from diagonal and off-diagonal components of the GF (26). Dispersion curves given by the maximum of the spectral function (41) in units of t along the symmetry directions $\Gamma(0,0) \to M(\pi,\pi) \to X(\pi,0) \to \Gamma(0,0)$ for $\delta = 0.1$ at $T = 0.03t$ are shown in figure 1, left panel. The dispersion reveals a rather flat hole-doped band (LHB in electron notation) at the Fermi energy (FE) ($\omega = 0$) and dispersing behavior far away from the FE. Our results for LHB resemble the dispersion curves obtained by LDA + DMFT numerical calculations for a model of $La_{2-\delta}Sr_\delta CuO_4$ by Weber et al. [31] despite a difference in hole concentrations. Their results are shown in figure 1, right panel, in the direction $\Gamma(0,0) \to X(\pi,0) \to K(\pi,\pi) \to \Gamma(0,0)$ in units of eV. The flat band crossing the FE is ascribed to the coherent QP excitations of the Zhang-Rice (ZR) singlet band, while the dispersing part is related to the incoherent ZR excitations related to the self-energy effects in DMFT. An abrupt change in the dispersion from the flat band to the dispersing part below the FE shown by white dashed lines in the right panel are associated with the so-called "waterfall" feature observed in ARPES experiments in cuprates. We also observe the "waterfall" feature, but, in contrast to [31], in our calculations the spectral intensity close $M(\pi,\pi)$ point is transferred to the UHB which is separated by a gap of the order of $U \sim 4t \sim \Delta_{pd}$ where Δ_{pd} is the charge-transfer gap in the LDA calculations in [31]. Most likely this difference is due to a momentum dependence of the self-energy (35) which is not accounted for in the DMFT calculations. There should also be taken into account a difference in the models (our two-subbands model versus three-band p-d model

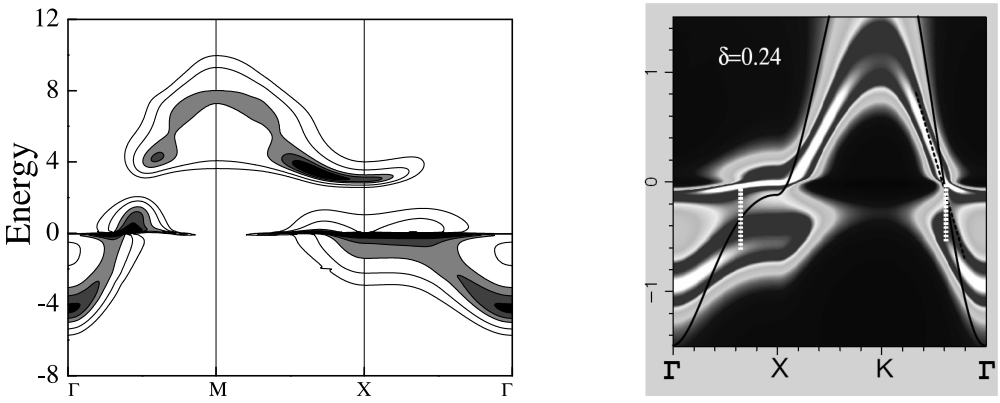

Figure 1. Dispersion curves in units of t for $\delta = 0.1$ (left panel) in comparison with LDA + DMFT calculations for $\delta = 0.24$ (right panel) [31].

in the LDA calculations) and a lower doping level in our calculations ($\delta = 0.1$ versus $\delta = 0.24$) which may result in different energy scales.

Studies of temperature and doping dependence of the spectral function (41) in [19] have revealed a strong increase of the dispersion and the intensity of the QP peaks at the Fermi energy in the overdoped region, $\delta = 0.3$, and at high temperature, $T = 0.3t$, which proves a strong effect of AF spin-correlations on the spectra. The obtained dispersion curves are in accord with numerical studies for the Hubbard model [6,7]).

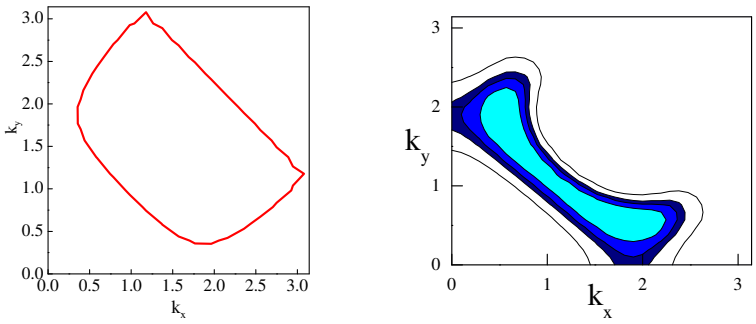

Figure 2. Fermi surface at $\delta = 0.05$ determined by the equation $\varepsilon_2(\mathbf{k}_\mathrm{F}) + \mathrm{Re}\,\Sigma(\mathbf{k}_\mathrm{F}, \omega = 0) = 0$ (left panel) and from maxima of the spectral function $A(\mathbf{k}, \omega = 0)$ (right panel).

Noticeable temperature and doping dependence was also observed for the Fermi surface (FS). Figure 2 shows the FS at hole doping $\delta = 0.05$ and $T = 0.03t$. In the left panel the FS determined by the equation: $\varepsilon_2(\mathbf{k}_\mathrm{F}) + \mathrm{Re}\,\Sigma(\mathbf{k}_\mathrm{F}, \omega = 0) = 0$ is represented by a large pocket. At the same time, the FS obtained from maxima of the spectral function $A_\mathrm{el}(\mathbf{k}, \omega = 0)$ on the (k_x, k_y)-plane shown in figure 2, right panel, reveals an arc-type shape with maximum intensity located on the large FS. This explains why in ARPES experiments, where the spectral function $A_\mathrm{el}(\mathbf{k}, \omega = 0)$ is measured, only this part of the FS has been detected (for a discussion see [32]). In the underdoped region $\delta < 0.05$ the hole pockets shrink while at higher doping the FS becomes open and in the overdoped region it transforms to an electron-like form. This FS transformation was confirmed by studying the electron momentum distribution function $N_{(\mathrm{el})}(\mathbf{k}) = 1 - N_{(h)}(\mathbf{k})$ where $N_{(h)}(\mathbf{k}) = \langle \sum_\sigma X^{\sigma\sigma}_\mathbf{k} + 2X^{22}_\mathbf{k} \rangle$ [19].

3.2. Equation for superconducting gap and T_c

In this subsection we discuss equations for the superconducting gap (36) and T_c at hole doping. For the linearized anomalous GF (37) the gap equation in the Matsubara frequency representation, $\omega_n = i\pi T(2n+1)$, can be written as

$$\begin{aligned}\varphi_{2,\sigma}(\mathbf{k}, i\omega_n) &= \frac{T}{N}\sum_{\mathbf{q}}\sum_{m}\Big\{ J(\mathbf{k}-\mathbf{q}) + \lambda^{(-)}(\mathbf{q}, \mathbf{k}-\mathbf{q} \mid i\omega_n - i\omega_m)\Big\} \\ &\times \; G_N^{22}(\mathbf{q}, -i\omega_m)\, G_N^{22}(\mathbf{q}, i\omega_m)\; \varphi_{2,\sigma}(\mathbf{q}, i\omega_m). \end{aligned} \tag{42}$$

Here the interaction function for the spin susceptibility model (38) is given by the equation

$$\lambda(\mathbf{q}, \mathbf{k}-\mathbf{q} \mid i\omega_\nu) = -|t(\mathbf{q})|^2\, \chi_s(\mathbf{k}-\mathbf{q})\, \frac{1}{\pi}\int_0^\infty \frac{2x\mathrm{d}x}{x^2 + (\omega_\nu/\omega_s)^2}\frac{1}{1+x^2}\tanh\frac{x\,\omega_s}{2T}\,. \tag{43}$$

To calculate T_c and to find the gap function one should find out the eigenvalue and the eigenfunction of the linear equation (42) in $(\mathbf{k}, \omega_n)$-space. In the strong-coupling limit within the Eliashberg-type theory, the full normal-state GFs (33), (34) self-consistently calculated taking into consideration the self-energy (35) should be used. A particular wave-vector dependence of the interaction (43) as a product of the $(\mathbf{q})$- and $(\mathbf{k}-\mathbf{q})$-dependent functions makes it possible to use the fast-Fourier transformation which helps to simplify the calculations. This program has been realized for the single-band t-J model in [14]. However, a complicated two-subband form of GFs (33), (34) in the Hubbard model presents a complicated problem for numerical calculations which has not been solved so far.

Therefore, as a first step, a weak-coupling approximation (WCA) for the gap function (42) can be considered. In the WCA the kernel of integral equation (36) is approximated by its value near the Fermi surface for energies $|\omega, z| \ll \mu$ as

$$K(\omega, z|\mathbf{q}, \mathbf{k}-\mathbf{q}) = -|t(\mathbf{q})|^2\, \chi(\mathbf{k}-\mathbf{q})\, \frac{1}{2}\tanh\frac{z}{2T}\,, \tag{44}$$

where $\chi(\mathbf{q}) = \mathrm{Re}\,\chi(\mathbf{q}, \Omega = 0)$ is the static susceptibility. In the WCA the self-energy contribution in the normal-state GF (34) is neglected which results in the following equation for the gap function at the Fermi energy $\Delta(\mathbf{k}) = \varphi_{2,\sigma}(\mathbf{k}, \omega = 0)$:

$$\begin{aligned}\Delta(\mathbf{k}) &= \frac{1}{N}\sum_{\mathbf{q}}\Big(J(\mathbf{k}-\mathbf{q}) - |t(\mathbf{q})|^2\,\chi(\mathbf{k}-\mathbf{q})\Big)\Big(\Big[\frac{(1-b(\mathbf{q}))^2}{2\varepsilon_2(\mathbf{q})} + \frac{b(\mathbf{q})(1-b(\mathbf{q})}{\varepsilon_1(\mathbf{q})+\varepsilon_2(\mathbf{q})}\Big]\,\tanh\frac{\varepsilon_2(\mathbf{q})}{2T} \\ &+ \Big[\frac{b(\mathbf{q})^2}{2\varepsilon_1(\mathbf{q})} + \frac{b(\mathbf{q})(1-b(\mathbf{q})}{\varepsilon_1(\mathbf{q})+\varepsilon_2(\mathbf{q})}\Big]\,\tanh\frac{\varepsilon_1(\mathbf{q})}{2T}\Big)\,\Delta(\mathbf{q}). \end{aligned} \tag{45}$$

In this equation, only the first term $\propto [(1-b(\mathbf{q}))^2/2\varepsilon_2(\mathbf{q})]\,\tanh(\varepsilon_2(\mathbf{q})/2T)$ shows a divergence on the FS for $\varepsilon_2(\mathbf{q}) \to 0$, while other terms with the energy $\varepsilon_1(\mathbf{q}) \sim U$ in denominators give much smaller contribution. This suggests that to estimate T_c, one can take into consideration only the contribution from the two-hole subband on the FS. A numerical solution of this reduced equation has been obtained in [21] in the limit of weak hybridization, $b(\mathbf{q}) \ll 1$. The d-wave pairing with high $T_c^{\max} \sim 200$ K was found. In the strong-coupling limit a certain reduction of $T_c^{\max}$ in comparison with WCA should be observed.

Concerning the mechanism of pairing in the Hubbard model, we can draw the following general conclusions from the gap equations (42) or (45). As follows from these equations, there are two channels of pairing. The first one is mediated by inter-subband hopping and is determined by the AF exchange interaction $J(\mathbf{k}-\mathbf{q})$ which is usually considered in the RVB-type theories [24]. There are no retardation effects for the exchange pairing due to a large hopping energy $U \gg t$ that results in the pairing of all electrons in the hole subband as shown in figure 3. The second contribution comes from the spin-fluctuation pairing $\propto \chi(\mathbf{k}-\mathbf{q})$ induced by intra-subband hopping which is only possible in a range of energies $\pm\omega_s$ near the FS, as in the BCS theory as sketched in figure 4.

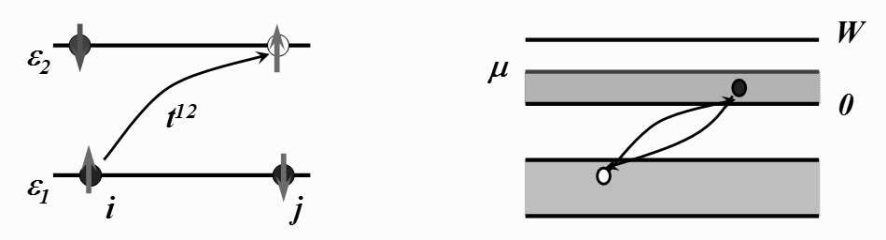

Figure 3. Antiferromagnetic exchange pairing mediated by inter-band hopping.

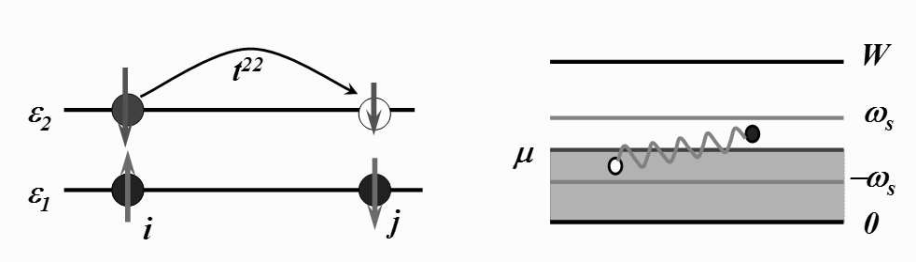

Figure 4. Spin-fluctuation pairing mediated by intra-band hopping.

The spin-fluctuation interaction is repulsive and can produce pairing only for a sign-varying gap on the FS, as the d-wave gap. This type of pairing is usually considered in phenomenological spin-fermion models [33].

To estimate both contributions, we consider the equation for the d-wave gap $\Delta(\mathbf{k}) = \Delta_0\,(\cos k_x - \cos k_y)/2 \equiv \Delta_0\,\eta(\mathbf{k})$ in the WCA in a conventional BCS form:

$$1 = \int\limits_{-\mu}^{\tilde{W}-\mu} \frac{\mathrm{d}\epsilon}{2\epsilon}\,\tanh\frac{\epsilon}{2T_{\mathrm{c}}}\,[J\,N_d(\epsilon) + \theta(\omega_s - |\epsilon|)\,\lambda_{\mathrm{sf}}\,N_s f(\epsilon)]\;, \tag{46}$$

where $N_d(\epsilon)$ and $N_{\mathrm{sf}}(\epsilon)$ are the density of electronic states for the exchange and spin-fluctuation interactions and the effective spin-fluctuation coupling constant is given by the hopping parameter averaged over the Fermi surface: $\lambda_{\mathrm{sf}} = \langle t^2(\mathbf{k})\,\eta^2(\mathbf{k})\rangle_{\mathrm{FS}}/\omega_s$ (for details see [21]). The integration over energy for the first term in (46) extends over all energies in the subband of the renormalized width $\tilde{W}$, while for the second term the integration is restricted as discussed above. By solving this equation in the standard logarithmic approximation, we derive for the superconducting T_{c} the following estimation

$$T_{\mathrm{c}} = \omega_s\,\exp(-1/\tilde{V}_{\mathrm{sf}}), \qquad \tilde{V}_{\mathrm{sf}} = V_{\mathrm{sf}} + \frac{V_{\mathrm{ex}}}{1 - V_{\mathrm{ex}}\ln(\mu/\omega_s)}\,, \tag{47}$$

where the effective coupling constants $V_{\mathrm{ex}} \sim J\,N_d(0)$ and $V_{\mathrm{sf}} \sim \lambda_{\mathrm{sf}}\,N_{\mathrm{sf}}(0)$. Even for a weak coupling, $V_{\mathrm{ex}} \sim V_{\mathrm{sf}} \sim 0.2$ a large value of T_{c} can be obtained by means of the enhancement of the spin-fluctuation coupling constant $\tilde{V}_{\mathrm{sf}}$ due to a large logarithm for $\mu \gg \omega_s$.

4. Conclusions

In the present paper a theory of superconducting pairing within the effective $p-d$ Hubbard model (2) with strong-electron correlations is presented. By employing the Mori-type projection technique for the equation of thermodynamic GFs [12] we obtained a self-consistent system for the matrix GF and the self-energies in the noncrossing approximation. The latter is similar to the Migdal-Eliasberg strong-coupling approximation.

It is important to point out that the investigations of models with strong electron correlations provide a microscopic theory for superconducting pairing mediated by the AFM exchange interaction and spin-fluctuation scattering induced by the kinematic interaction, characteristic of the systems with strong correlations. These mechanisms of superconducting pairing are absent in the fermionic models (for a discussion, see Anderson [34]) and they appear to be generic for cuprates. The singlet $d_{x^2-y^2}$-wave superconducting pairing was proved for the original two-band p-d Hubbard model. Therefore, we believe that the proposed magnetic mechanism of superconducting pairing is a relevant mechanism of high-temperature superconductivity in copper-oxide materials.

Acknowledgements

One of the authors (N.P.) is grateful to Prof. P. Fulde for the hospitality extended to him during his stay at MPIPKS, Dresden, where a major part of the present work has been done.

References

1. Hubbard, J., Proc. Roy. Soc. A (London), 1963, **276**, 238.
2. Dagotto, E., Rev. Mod. Phys., 1994, **66**, 763.
3. Bulut N., Adv. Phys., 2002, **51**, 1587.
4. Georges A., Kotliar G., Krauth W., Rozenberg M., Rev. Mod. Phys., 1996, **68**, 13.
5. Kotliar G., Savrasov S.Y., Haule K., Oudovenko V.S., Parcollet O., Marianetti C.A., Rev. Mod. Phys., 2006, **78**, 865.
6. Maier Th., Jarrel M., Pruschke Th., Hettler M.H., Rev. Mod. Phys., 2005, **77**, 1027.
7. Tremblay A.-M.S., Kyung B., Sénéchal D., Fiz. Nizk. Temp. [Sov. J. Low Temp. Phys.], 2006, **32**, 561.
8. Plakida N.M., Fiz. Nizk. Temp. [Sov. J. Low Temp. Phys.], 2006, **32**, 483.
9. Hubbard, J., Proc. Roy. Soc. A (London), 1965, **285**, 542.
10. Zaitsev R.O., V.A. Ivanov, Soviet Phys. Solid State, 1987, **29**, 2554; Ibid., 1987, **29**, 3111; Int. J. Mod. Phys. B, 1988, **5**, 153;
11. Plakida N.M., Stasyuk I.V., Modern Phys. Lett., 1988, **2**, 969.
12. Zubarev D.N., Usp. Fiz. Nauk, 1960, **71**, 71; Usp. Fiz. Nauk [Sov. Phys. – Usp.] , 1960, **3**, 320); Nonequilibrium Statical Thermodynamics. Consultant Bureau, New-York, 1974.
13. Plakida N.M., Yushankhai V.Yu., Stasyuk I.V., Physica C, 1989, **160**, 80; Yushankhai V.Yu., Plakida N.M., Kalinay P., Physica C, 1991, **174**, 401.
14. Plakida N.M., Oudovenko V.S., Phys. Rev. B, 1999, **59**, 11949.
15. Beenen J., Edwards D.M., Phys. Rev. B, 1995, **52**, 13636.
16. Avella A., Mancini F., Villani D., Matsumoto H., Physica C, 1997, **282–287**, 1757; Di Matteo T., Mancini F., Matsumoto H., Oudovenko V.S., Physica B, 1997, **230–232**, 915.
17. Stanescu T.D., Martin I., Phillips Ph., Phys. Rev. B, 2000, **62**, 4300.
18. Plakida N.M., Hayn R., Richard J.-L., Phys. Rev. B, 1995, **51**, 16599.
19. Plakida N.M., Oudovenko V.S., Sov. Phys. – JETP, 2007, **104**, 230.
20. Plakida N.M., Physica C, 1997, **282–287**, 1737.
21. Plakida N.M., Anton L., Adam S., Adam Gh., Zh. Exp. Theor. Fyz, 2003, **124**, 367 [JETP, 2003, **97**, 331].
22. Zhang F.C., T.M. Rice, Phys. Rev. B, 1988, **37**, 3759.
23. Feiner L.F., Jefferson J.H., Raimondi R., Phys. Rev. B, 1996, **53**, 8751.
24. Anderson P.W., Science, 1987, **235**, 1196; The theory of superconductivity in the high-T_c cuprates. Princeton University Press, Princeton (1997).
25. Eliashberg G.M., Zh. Eksp. Teor. Fiz., 1960, **38**, 966; ibid., 1960, **39**, 1437 [Sov. Phys. – JETP, 1960, **11**, 696; ibid., 1960, **12**, 1000].
26. Migdal A.B., Zh. Eksp. Teor. Fiz., 1956, **34**, 1438, [Sov. Phys. – JETP, 1958, **7**, 996].
27. Liu Z., Manousakis E., Phys. Rev. B, 1992, **45**, 2425.
28. Jaklič J., Prelovśek P., Phys. Rev. Lett., 1995, **74**, 3411; ibid., 1995, **75**, 1340.
29. Bonca J., Prelovśek P., Sega I., Europhys. Lett., 1989, **10**, 87.
30. Korshunov M.M., Gavrichkov V.A., Ovchinnikov S.G., Nekrasov I.A., Pchelkina Z.V., Anisimov V.I., Phys. Rev. B, 2005, **72**, 165104.
31. Weber C., Haule K. , Kotliar G. Preprint arXiv:cond–mat/0804.1512, 2008.

32. Kuchinskii E.Z., Nekrasov I.A., Sadovskii M.V., Fiz. Nizk. Temp. [Sov. Phys. – J. Low Temp. Phys.], 2006, **32**, 528.
33. Chubukov A., Pines D., Schmalian J. A spin fluctuation model for *d*-wave superconductivity. – In: Handbook of Superconductivity. Conventional, high-transition temperature, and novel superconductors, Eds.: Benemann, K.H., Ketterson, J.B., (Springer, Berlin,) 2002.
34. Anderson P.W., Adv. Phys., 1997, **46**, 3.

Електронний спектр і надпровідність в моделі Хаббарда

М.М.Плакіда[1,2], В.С.Удовенко[1,3]

[1] Об'єднаний інститут ядерних досліджень, 141980 Дубна, Росія
[2] Інститут Макса Планка з фізики складних систем, Дрезден 01187, Німеччина
[3] Університет Ратгерса, Піскатавей, Нью-Джерсі 08854, США

Отримано 20 травня 2008 р., в остаточному вигляді – 10 червня 2008 р.

В рамках моделі Хаббарда, сформульовано мікроскопічну теорію електронного спектру та надпровідного спарювання. З використанням техніки проектування типу Морі, отримано рівняння Дайсона для нормальних і аномальних функцій Ґріна побудованих на операторах Хаббарда. Власноенергетична частина розрахована в наближенні без перетинів для розсіяння електронів на спінових і зарядових флуктуаціях, які створюються кінематичною взаємодією для операторів Хаббарда. Приведені чисельні результати для електронної дисперсії в границі сильних кореляцій. Обговорюється можливість надпровідного спарювання через антиферомагнітні обмінні та спінові флуктуації.

Ключові слова: *сильні електронні кореляції, модель Хаббарда, надпровідність*

PACS: *74.20.Mn, 71.27.+a, 71.10.Fd, 74.72.-h*